PHENOMENOLOGICAL AND SEMIMICROSCOPIC ANALYSIS OF 50-MeV ALPHA PARTICLES SCATTERING AND STRUCTURE OF EVEN TIN ISOTOPES

K.A. KUTERBEKOV, I.N. KUCHTINA[1], B.M. SADYKOV, E.I. ISMATOV[2]

UDC 539.143/.144

Institute of Nuclear Physics, Nat. Nuclear Center of Kazakhstan
(1, Ibragimov Str., Almaty 48082, Republic of Kazakhstan; e-mail: kuterbekov@inp.kz),

[1]**Joint Institute for Nuclear Research**
(Dubna 141980, Moscow Region, Russian Federation),

[2]**Institute of Nuclear Physics, Acad. Sci. of Uzbekistan**
(Ulugbek, Tashkent 702132, Uzbekistan Republic)

A phenomenological and semimicroscopic analysis of data derived in experiments on elastic and inelastic scattering of 50-MeV alpha particles resulted from their collisions with ^{112,114,120,124}Sn nuclei has been carried out (with attraction of available data on complete cross sections of reactions) within the framework of the optical potential approach and techniques of distorted waves and coupled channels. For the low-lying 2_1^+ и 3_1^- states, corresponding values of deformation parameters, deformation lengths, and the ratios of neutrons and protons multipolar transition matrix elements are obtained and a comparison between the obtained parameters and published data is carried out for other types of the projectile particles.

Introduction

The substance distribution in a nucleus is studied by using a scattering of strongly interacting alpha particles. A detailed information on the distribution of the proton component in a nucleus is obtained by using the Coulomb excitation of nuclei and scattering of electrons [1]. Comparison between these experiments allows the investigation of differences in the neutron and proton distributions of nuclei and their structure. Isospin character of excited states of zirconium even isotopes is comprehensively studied in works [2—4] by using the scattering of alpha particles. However, the same interrogation has not been done for Sn isotopes [5, 6].

Parameters of the optical potential (OP) of the interaction between alpha particles and medium nuclei for low and intermediate energies, which can be extracted from analysis of the angle distribution of differential cross sections (ADDCS) of elastic scattering within the frame of the optical model (OM), are susceptible to ambiguity. A combined analysis of the ADDCS of elastic scattering and the total cross sections of reactions (TCSR) allows the limitation of ambiguities of the OP parameters, since the data on differential and total cross sections are the main nuclear values obtained from the OM. Up to now, few works have been completed in which both the ADDCS of scattering and TCSR were involved. A choice of optimal parameters of OP will allow, in the future, the derivation of a substantiated information on the structure of the excited states of a nucleus under study. The semimicroscopic analysis of the data on "alpha particles — Sn" quasielastic scattering has been carried out rarely.

In this work, the results of measurements of the angular distribution of alpha particles scattered elastically and inelastically by ^{112,114,120,124}Sn atoms are presented. The measurements were conducted at an isochronous cyclotron U-150M located in Kazakhstan. Within the frame of a unified approach, the joint analysis of the data on quasielastic scattering of 40- and ∼50-MeV alpha particles by even Sn isotopes has been conducted along with the analysis of available TCSR data. The data were analyzed by using models of deformed potential of the OM and the methods of coupled channels (CCM), distorted-wave Born approximation (DWBA), and semimicroscopic folding model (SMFM). A comparative analysis of the deformation lengths δ_2^N and δ_3^N of low-lying states of the investigated nuclei and the ratios of neutron-proton multipole matrix elements M_n/M_p obtained in this work and from available publications is conducted by taking into consideration various types of projectile particles and using various analysis techniques.

Experimental Technique

The experiment has been performed with employment of a cyclotron U-150M of the Nuclear Physics Institute

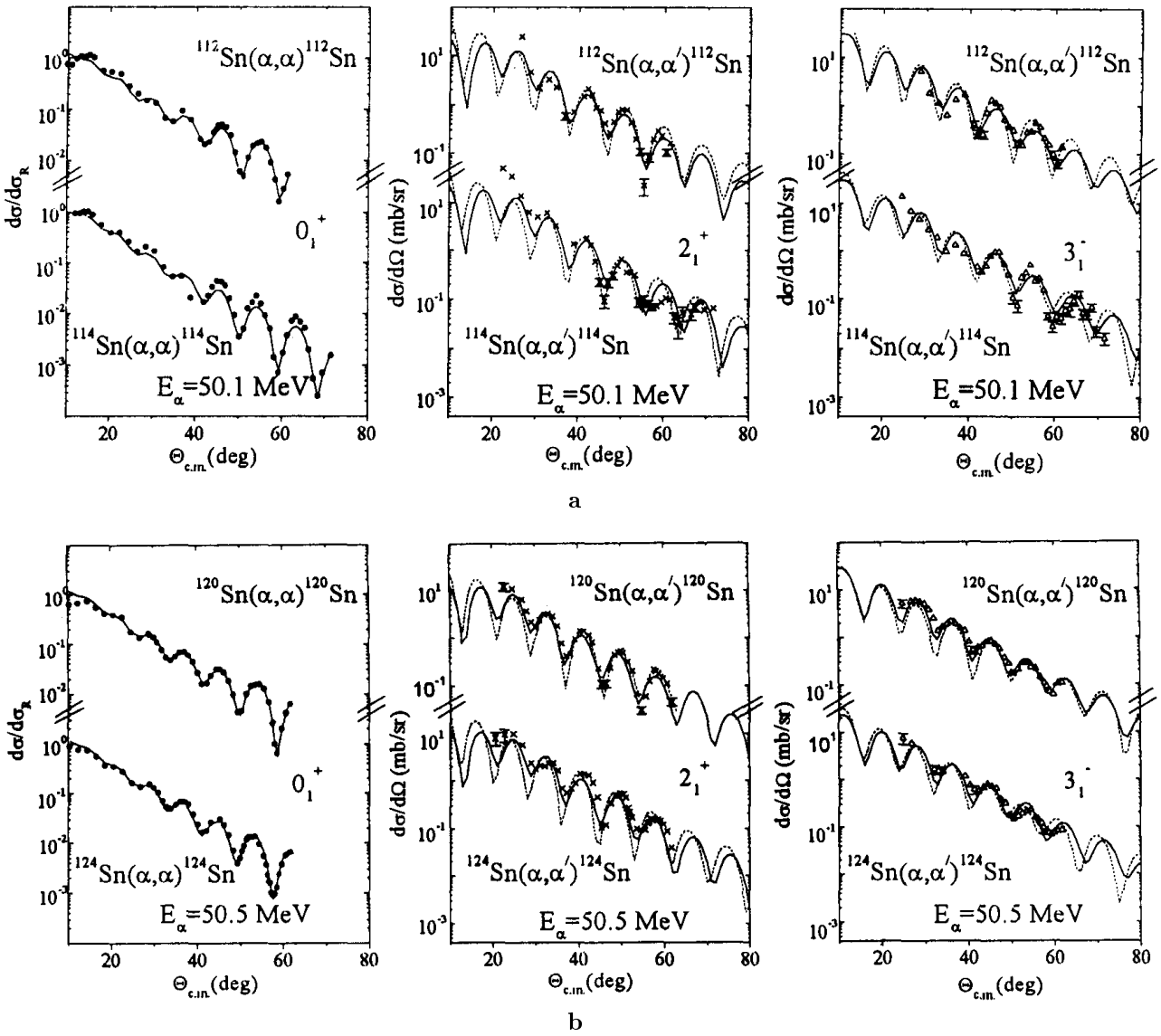

Fig. 1. Angular distributions of the elastic and inelastic scattering of projectile alpha particles colliding with ^{112,114}Sn (*a*) and ^{120,124}Sn (*b*) nuclei (the symbols denote experimental data, and the solid line — optical model for the elastic channel (0^+) and phenomenological MCC analysis for 2^+_1 and 3_1 states, and the dotted line shows the DWBA data) at E_α=(50.1± 0.5) MeV

(Almaty, Kazakhstan). Alpha particles have been accelerated to the energies of (50.1±0.5) and (50.5±0.5) MeV.

A ($\Delta E - E$) technique based on the principle of fast-slow coincidences in semiconductor detectors was employed. 100- to 200-μm-thick detectors were used as ΔE counters, whereas the total absorption was measured with 1- to 2-μm thick diffusion-drift Si (Li) detectors. Other details of the experimental setup are given in work [8].

As a target, self-sustaining foils made of Sn isotopes were used; their thicknesses and isotope enrichment values are presented in Table 1.

T a b l e 1. Thickness and isotope concentration of Sn targets

Alpha particles energy, MeV	Target	Target thickness, mg/cm^2	Isotope content, %
50.1 ± 0.5	^{112}Sn	1.42 ± 0.08	75.0
50.1 ± 0.5	^{114}Sn	1.82 ± 0.08	60.0
50.5 ± 0.5	^{120}Sn	2.20 ± 0.08	99.2
50.5 ± 0.5	^{124}Sn	2.00 ± 0.08	95.1

T a b l e 2. Optical potential parameters for elastic scattering of near-50-MeV alpha particles colliding with ^{112,114,120,124} Sn nuclei.

Nucleus	E_α, MeV	V, MeV	W, MeV	a_v fm	a_w, fm	σ_R, mb	$J_R/4A$, MeV· fm^{-3}	χ^2
^{112}Sn	50.1	156.89	21.728	0.757	0.547	1959	367	6.8
^{114}Sn	50.1	148.63	17.351	0.773	0.632	1957	349	8.3
^{120}Sn	50.5	147.55	15.619	0.748	0.584	1800	341	2.7
						1768 ± 78[11]		
^{124}Sn	50.5	149.46	16.192	0.762	0.665	1900	330	2.6

The differential cross sections of elastic and inelastic scattering of alpha particles are measured in the angle range of 10—65° (lab) with an angle step from 0.4 to 1°. Errors in the determination of absolute values of the cross sections constituted 3—8% for the elastic channel and 7—20% for the inelastic one. The complete angle resolution of the alpha spectrometer was measured by a technique developed in [8] and turned out to be 0.3°. It is shown that the mean systematic angle error $\delta\,\theta$ caused by a lack of coincidence between the chamber axis and the beam of projectile particles constituted 0.5°, thus requiring to be specially measured in every series of the experiments. Experimentally measured ADDCS values for the scattering of alpha particles are shown in Fig. 1.

Experimental Data Analysis

1. Phenomenological Optic-Potential Approach and Method of Coupled Channels and Distorted Waves

The data on elastic scattering of about 50-MeV alpha particles colliding with ^{112,114,120,124}Sn isotopes are analyzed by using the deformed potential of OM. Theoretical calculations have been conducted within the frame of the SPI-GENOA program [9]. As the starting parameters of OP, the data of work [10], in which the global dependences of the OM parameters for the case of scattering of up-to-80-MeV alpha particles are presented, were used. The OP parameters have been selected to achieve a best accordance between the theoretical and experimental angle distributions of the elastic scattering, on the one hand, and the corresponding TCSR values, on the other one. The search for optimal OP parameters has been carried out by minimizing χ^2/N value. The Coulomb radius was accepted to be $r_C = 1.25$ fm. The obtained values of the OP parameters, χ^2/N values, volume integral J_R, total cross section σ_R (both the calculated and experimental [11] ones for ^{120}Sn) of the reactions are presented in Table 2. Note that the TCSR values resulted from our calculations with the use of potential parameters of Table 2, coincide with experimental data of work [12] and with the regularities of TCSR variations exhibited there for the case of Sn isotopes.

An analysis of ADDCS of inelastic scattering has been performed with the DWUCK4 program [13] within the frame of DWBA by using a formfactor of the collective vibration model, and within the frame of CCM — by using the vibration approximation of the ECIS-88 program [14].

The results of fitting the theoretical curves to the experimental ADDCS values of elastic and inelastic channels of the scattering of projectile alpha particles by ^{112,114,120,124}Sn nuclei within the frame of the phenomenologycal OP approach are presented in Fig. 1.

2. Semimicroscopic Analysis of Experimental Data

In the semimicroscopic approach, optical potential $U(R)$ is constructed within the frame of the folding model, on the basis of the total M3Y effective interaction and nucleonic densities calculated by the method of density matrix functional [15]. The potential of interaction between two colliding nuclei, in the first order of effective forces, can be represented as a sum

$$U(R) = U^E(R) + U^D(R), \tag{1}$$

where $U^D(R)$ is the "direct" potential of the double convolution model [16]:

$$U^D(R) = \int\int \rho^{(1)}(r_1) V^D(s) \rho^{(2)}(r_2) dr_1 dr_2. \tag{2}$$

In expression (2), $V^D(s)$ is the "direct" component of the effective interaction ($s = r_2 - r_1 + R$), and $\rho^{(i)}(r_i)$ are the densities of colliding nuclei ($i = 1, 2$). A similar scheme of calculation of the exchange potential $U^E(R)$ is given in work [17]. The effects of single-nucleon exchange give the main contribution to the

scheme and can be described with employment of the density-matrix formalism [18]:

$$U^{\rm ex}(R) = \int\int \rho^{(1)}(r_1, r_1 + s) V_{\rm ex}(s) \rho^{(2)}(r_2, r_2 - s) \times$$

$$\times \exp(ik(R)s/\eta) dr_1 dr_2, \qquad (3)$$

where $V_{\rm ex}(s)$ is the exchange component of the effective nucleon-nucleon forces, $\rho^{(i)}(r,r')$, $(i = 1, 2)$ are the density matrices of colliding nuclei with mass numbers A_1 and A_2, and $k(R)$ is a local momentum of the relative motion of nuclei, which is determined from the relationship

$$k^2(R) = (2m\eta/h^2)[E - U(R) - V_{\rm C}(R)]. \qquad (4)$$

Here, $\eta = A_1 A_2/(A_1 + A_2)$, $s = r_2 - r_1 + R$, E is the energy in a center of mass system, and $V_{\rm C}(R)$ is the Coulomb potential. Thus, the potential resulted from the account of the effects of the single-nucleon exchange, depends on energy. As input data for the potential calculation, effective nucleon-nucleon forces are taken along with the proton and neutron densities of colliding nuclei.

The complete optical potential should include, besides a real part, also an imaginary one describing the absorption of an incoming particle into inelastic channels. In our case, the absorption potential was built as being dependent on the calculated real part in the form [19]

$$W(R) = i[N_w U(R) - \alpha_w R dU(R)/dR] \qquad (5)$$

where $U(R)$ is the double-convolution potential (1), and N_w and α_w are parameters characterizing, respectively, the volume and superficial components of the absorption potential. A surface-related component simulating a contribution of the dynamic polarization potential is added to the real part of the potential [20]. The complete optical potential takes form

$$U_t(R) = U(R) - \alpha_v(dU(R)/dR) +$$

$$+ i[N_w U(R) - \alpha_w(dU(R)/dR)], \qquad (6)$$

where α_v, N_w, and α_w are variable parameters.

In the calculation of the cross sections of inelastic scattering, the formfactor of inelastic transition was taken as $\alpha_L(dU_t(R)/dR)$ [21].

Within the frame of SMFM, an analysis of differential cross sections of elastic and inelastic scattering has been carried out along with TCSR of alpha particles colliding with even-even Sn isotopes with energies of 40, 50.1, and 117.2 MeV. The experimental data on elastic and inelastic scattering of near-50-MeV alpha particles colliding with isotopes ^{112}Sn, ^{114}Sn, ^{120}Sn, and ^{124}Sn are taken from the present work, and the data for a nucleus ^{120}Sn at 40-MeV energy of alpha particles — from work [7]. For the analysis of TCSR, the data of works [11, 12] were used. Potentials of SMFM were built according to the above scheme. In Table 3, root-mean-square radii of the density distributions of protons, neutrons, and a substance, for alpha particles and Sn isotopes with mass numbers $A = 112$, 114, 120, 124, are presented.

In Tables 4 and 5, there are presented the integral characteristics of potentials for the investigation of the channels of interaction between alpha particles and Sn isotopes within the frame of SMFM. It is seen from Table 4 that the volume integral J_R increases in its absolute value with the mass number at a fixed energy E_α of a projectile particle, and decreases in its absolute value if E_α rises at a fixed A. The root-mean-square radii (Table 5) of the folding potentials experience a rise if A

Table 3. Root-mean-square radii (measured in fm) of the density distributions of protons, neutrons, and a substance. Also, differences $\Delta r_{np} = \langle r_n^2\rangle^{1/2} - \langle r_p^2\rangle^{1/2}$ are presented

Nucleus	$\langle r_n^2\rangle^{1/2}$	$\langle r_p^2\rangle^{1/2}$	$\langle r_m^2\rangle^{1/2}$	Δr_{np}
^{4}He	1.570	1.570	1.570	0.000
^{112}Sn	4.537	4.591	4.567	0.054
^{114}Sn	4.555	4.627	4.596	0.072
^{120}Sn	4.602	4.726	4.675	0.124
^{124}Sn	4.628	4.782	4.720	0.154

Table 4. Volume integrals of the folding potentials (in 10^3 MeV·fm^3)

System	E_α, MeV		
	40.0	50.1	117.2
^{4}He+^{112}Sn	−147.2	−145.1	−132.2
^{4}He+^{114}Sn	−149.8	−147.7	−134.6
^{4}He+^{120}Sn	−157.6	−155.4	−141.6
^{4}He+^{124}Sn	−162.7	−160.4	−146.1

Table 5. Root-mean-square radii (in fm) of the folding potentials

System	E_α, MeV		
	40.0	50.1	117.2
^{4}He+^{112}Sn	5.210	5.210	5.217
^{4}He+^{114}Sn	5.237	5.237	5.244
^{4}He+^{120}Sn	5.310	5.310	5.316
^{4}He+^{124}Sn	5.352	5.353	5.358

increases at a certain E_α value, whereas the radii vary just slightly for a fixed A if the energy of alpha particles increases.

In Table 6, there are presented optimal values of the folding model parameters α_v, N_w, and α_w (see formulae (5) and (6)), under which the experimentally obtained ADDCS values of elastic and inelastic scattering are described with an acceptable accuracy, if low-level (2_1^+ and 3_1^-) states are excited, and TSCR values. It is seen from Table 6 that values of the SMFM parameters are practically the same for different Sn isotopes (with increase of the number of neutrons), instead, they depend only on the energy E_α of projectile particles. In Table 6, the parameters N_w, α_v, and α_w that characterize the volume- and surface-related components of the absorption potential are presented; δ_l^N is the deformation length.

In Figs. 2 and 3, the fitting results for predicted (using SMFM) and experimental differential sections of alpha particles colliding with Sn isotopes are presented. A good agreement is achieved between the predicted values and the experimentally obtained ADDS's for elastic scattering and inelastic (2_1^+ and 3_1^-) channels under weakly varying parameters N_w, α_v, and α_w in the considered range of energies.

In Table 7, calculated CSR values σ_R^{theor} are presented for the investigated Sn isotopes for different energies of alpha particles, as well as available experimental data on TCSR, σ_R^{exp}, for energies of 23.25, 27.8, 40, and 117.2 MeV cited from works [22, 11, 12]. For a system $\alpha+^{120}$Sn subjected to bombardment of 40-MeV alpha particles, the parameters of potential used in the TCSR calculation were taken with accounting for the (good-described) experimental ADDCS values, therefore, the mentioned total cross section value can be considered, with a high probability, as a reliable one. In all cases, the preceding experience [4] as to choosing a value of the potential parameter has been taken into account. For 23.25-MeV alpha particles, TCSR for the case of collisions with a ^{120}Sn nucleus, calculated using SMFM, turned out to be by 6% lower than the experimental value.

If one takes into account the inaccuracies of theoretical TCSRs σ_R^{theor} obtained in this work within the SMFM frame, and the experimental total cross sections σ_R^{exp} taken from Table 7 and accounting for their dependence on energy [22, 11, 12], then the comparison can be considered as good. In this case, also the dependence on energy of these values, including σ_R, is taken into account. This fact confirms once more an adequacy of the predicted cross sections calculated with the use of the above-described semimicroscopic approach.

Results and Discussion

In Table 8, there are presented the values of reduced electric transient probabilities $B(EL)$, deformation parameters β_l, deformation lengths δ_l^N, and the ratios of neutron-proton multipole matrix elements M_n/M_p of low-lying states of the investigated Sn nuclei, obtained in the present analysis and other analysis techniques described in the literature sources. Here, we present the information related to various types of projectile particles (α, p, e, and others) that are more or less sensitive to the neutron and proton components of the deformation lengths and M_n/M_p ratios.

When conducting a comparative analysis of the data of Table 8, we have taken into account the methods of obtaining the data, reliability of the data, and their appropriateness for the comparison. In particular, δ_2^N values obtained by DWBA at $E_\alpha = 44.0$ MeV [24] with using the Austern—Blair model, are underestimated and not exceed the corresponding values obtained using the optic-potential methods DWBA and CCM. At the same time, within the frame of a certain method of analysis, the data on $B(EL)$, β_l, and deformation lengths δ_2^N

T a b l e 6. Values of the semimicroscopic potential parameters and deformation lengths for Sn isotopes

Target nucleus	E_α, MeV	α_ν	N_w	a_w	δ_l^N, fm	
					2_1^+	3_1^-
^{112}Sn	50.1	–0.02	0.20	0.01	0.758	0.658
^{114}Sn	50.1	–0.02	0.20	0.01	0.763	0.662
^{120}Sn	40.0	–0.03	0.20	0.01	0.743	0.673
	50.5	–0.01	0.20	0.01	0.743	0.603
^{124}Sn	50.5	0.00	0.20	0.01	0.750	0.859

T a b l e 7. Parameters of the semimicroscopic model and total cross sections of reactions for the scattering of alpha particles colliding with Sn isotopes

Nucleus	E_α, MeV	α_v	N_w	α_w	σ_R^{theor}, mb	σ_R^{exp}, mb
^{112}Sn	40.0	–0.02	0.20	0.01	1743	
	50.1	—0.02	0.20	0.01	1892	
	117.2	0.00	0.20	0.01	2145	2140±160 [12]
^{114}Sn	40.0	–0.03	0.20	0.01	1766	
	50.1	–0.02	0.20	0.01	1910	
	117.2	0.00	0.30	0.02	2169	
^{120}Sn	23.25	–0.05	0.20	0.02	1285	1367±47 [22]
	27.8	–0.03	0.20	0.01	1486	1509±45 [22]
	40.0	–0.02	0.20	0.01	1830	1768±78 [11]
	50.1	–0.01	0.20	0.01	1952	
	117.2	0.00	0.30	0.02	2227	2360±150 [12]
^{124}Sn	40.0	0.00	0.20	0.01	1808	
	50.1	0.00	0.20	0.01	1991	
	117.2	0.00	0.30	0.02	2278	2340±160 [12]

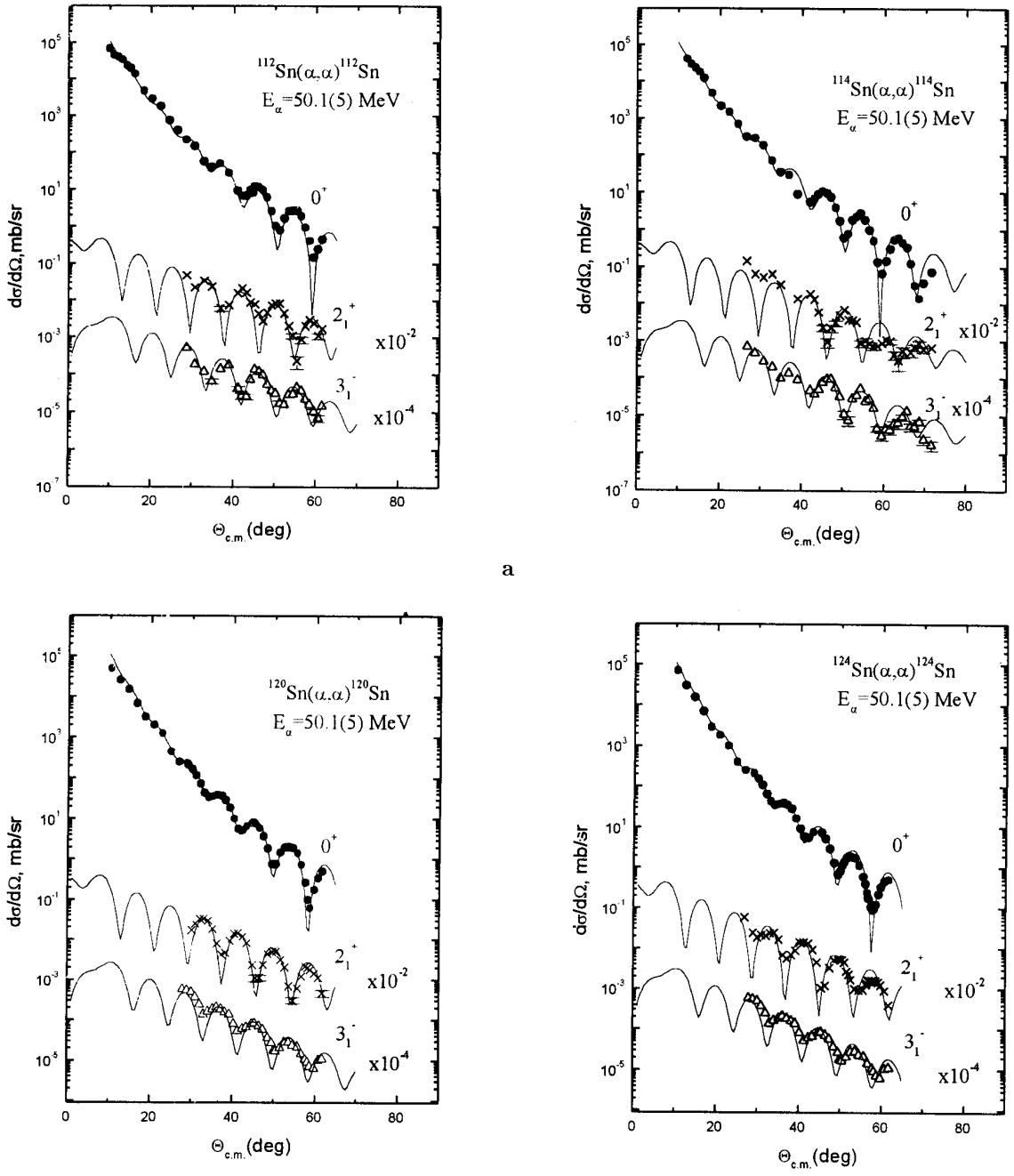

Fig. 2. Angular distributions of the differential cross sections of elastic and inelastic scattering of alpha particles colliding with ^{112,114}Sn (a) and ^{120,124}Sn (b) nuclei (the symbols show the experimental data, and the solid curves — the results of semimicroscopic analysis) with $E_\alpha = (50.1 \pm 0.5)$ MeV

taken from work [26] for the 2_1^+state of ^{112}Sn nucleus, coincide with values of work [25].

In work [27], $B(E2)$ are lesser by 6 or 9 percent than those in works [28, 29], but, because of their high errors, the $B(E2)$ values and deformation lengths overlap with one another. In works [28, 29], $B(E2)$ and δ_2^N values for Sn isotopes are in satisfactory agreement. The observed discrepancies can be explained by different experimental

conditions (there were applied different techniques: a "pure" Coulomb excitation or a measurement of the inelastic scattering with coincidence of gamma quanta, different enrichment of the targets, etc.).

In works [7, 30], β_l values were obtained using the DWBA method for 2_1^+ and 3_1^- states of ^{120}Sn nucleus from scattering measurements for 40- and 34.4-MeV alpha particles, correspondingly. In [7, 30], for the formfactor of Woods—Saxon type, radii of the real and imaginary parts of OP are taken to be equal to one another, whereas the deformation lengths are not determined, although values of the deformation parameters are in acceptable agreement with our data.

T a b l e 8. Comparative data for N/Z, $B(EL)$, β_l, δ_l^N and M_n/M_p values for ^{112,114,120,124}Sn isotopes

Isotopes N/Z	Energy of the state, MeV	$B(EL)$, (e^2b^l)	β_l	δ_l^N, fm	(Particle, energy (MeV)) methods	M_n/M_p	Reference
1	2	3	4	5	6	7	8
				2_1^+ state			
			0.140(11)	0.758(60)	(α,50.1) CC,SMA	1.385	this work
^{112}Sn			0.130(11)	0.780(70)	(α,50.1) CC	1,454	this work
1.24	1.250		0.151(14)	0.906(89)	(α,50.1) DWBA		this work
		0.289(14)	0.135(7)	0.781(39)	(α,10.07) Coulomb Excit.		[23]
		0.0457		0.70(7)	(α,44) A.-B.-DWBA		[24]
			0.152(10)	0.879(88)	(p,16) DWBA		[25]
		0.492(34)	0.143(5)	0.87(3)	(p,20.5) DWBA		[26]
			0.136(5)		(p,20.5) CC		[26]
		0.18(4)	0.130	0.614(135)	Coulomb Excit.		[27]
		0.229(5)		0.693(15)	(α,10.6) Coulomb Excit.		[28]
		0.256(6)		0.732(17)	(α,10) Coulomb Excit.		[29]
			0.140(11)	0.763(61)	(α,50.1) CC,SMA	1.510	this work
^{114}Sn			0.120(10)	0.724(65)	(α,50.1) CC	1.382	this work
1.28	1.260		0.130(11)		(α,50.1) DWBA		this work
		0.20(7)	0,118	0.693(242)	Coulomb Excit.		[27]
		0.0420		0.67	(α,44) A.-B.-DWBA		[24]
			0.139(10)	0.743(57)	(α,40, 50.5) CC,SMA	1,817	this work
^{120}Sn			0.101(9)	0.620(50)	(α,50.5) CC	1.351	this work
1.40	1.180		0.106(9)	0.650(52)	(α,50.5) DWBA		this work
			0.109(10)		(α,34.4) DWBA		[30]
			0.12(2)		(α,40) DWBA		[7]
			0.12		(n,46)		[31]
		0.170(40)	0.112	0.584(137)	Coulomb Excit.		[27]
		0.0247(41)			(e,150) B_I(L→0)		[32]
			0.113	0.667(35)	(p,16) CC		[33]
			0.119(10)	0.704(64)	(p,16) DWBA		[25]
			0.12	0.653	(d,15) DWBA		[34]
		0.044		0.66	(α,44) A.-B.-DWBA		[24]
		0.230(12)	0.115(6)	0.681(34)	(α,10.07) Coulomb Excit.		[23]
			0.129(4)	0.713(25)	(p,24.5) DWBA		[35]
		0.197(4)		0.628(13)	(α,10.0) Coulomb Excit.		[28]
		0.203(4)		0.638(13)	(α,10) Coulomb Excit.		[29]
			0.13(1)		(p,17.8) DWBA		[36]
			0.140(12)	0.750(60)	(α,50.5) CC,SMA	2.266	this work
^{124}Sn			0.096(9)	0.595(54)	(α,50.5) CC	1.591	this work
1.48	1.130		0.100(9)	0.620(60)	(α,50.5) DWBA		this work
		0.140(6)	0.082(2)	0.491(10)	(α,19.5) Coul.-Nucl.Interf.		[37]
		0.0266(45)			(e,150) B_I(L→0)		[32]
			0.119(4)	0.640	(p,24.5) DWBA		[35]
				0.528(35)	(p,16) CC		[33]
			0.108(7)	0.646(60)	(p,16) DWBA		[25]
		0.150(30)	0.108	0.542(108)	Coulomb Excit.		[27]
		0.051		0.71	(α,44) A.-B.-DWBA		[24]
		0.184(9)	0.101(5)	0.604(30)	(α,10.07) Coulomb Excit.		[23]
		0.170(4)		0.577(14)	(α,10.0) Coulomb Excit.		[28]
		0.161(4)		0.562(14)	(α,10) Coulomb Excit.		[29]

(*Continuation*)

1	2	3	4	5	6	7	8
				3_1^- state			
			0.144(12)	0.658(56)	(α,50.1) CC,SMA		this work
^{112}Sn			0.140(13)	0.840(80)	(α,50.1) CC		this work
1.24	2.350		0.155(16)	0.930(98)	(α,50.1) DWBA		this work
		0.00705		0.56	(α,44) A.-B.-DWBA		[24]
			0.203(10)	1.174(164)	(p,16) DWBA		[25]
		0.251(18)	0.146(5)	0.96(3)	(p,20.5) DWBA		[26]
			0.133(5)	0.805(5)	(p,20.5) CC		[26]
			0.144(13)	0.662(66)	(α,50.1) CC,SMA		this work
^{114}Sn			0.120(11)	0.724(70)	(α,50.1) CC		this work
1.28	2.300		0.130(13)	0.784(85)	(α,50.1) DWBA		this work
		0.16(6)		0.099(40)	(N14,52.5)Coulomb Excit.		[38]
		0.0088		0.62	(α,44) A.-B.-DWBA		[24]
			0.141(12)	0.673(59)	(α,40) CC,SMA		this work
^{120}Sn			0.129(11)	0.603(50)	(α,50.5) CC,SMA		this work
1.40	2.390		0.132(12)	0.810(77)	(α,50.5) CC		this work
			0.119(11)	0.730(70)	(α,50.5) DWBA		this work
			0.120(10)		(α,34.4) DWBA		[30]
			0.14(3)		(α,40) DWBA		[7]
			0.17		(n,46)		[31]
		0.0162(20)			(e,150) B_I(L$\to$0)		[32]
			0.151	0.892(38)	(p,16) CC		[33]
			0.159(20)	0.941(133)	(p,16) DWBA		[25]
			0.14	0.762	(d,15) DWBA		[34]
		0.0098		0.62	(α,44) A.-B.-DWBA		[24]
		0.13(5)			(N14,52.5)Coulomb Excit.		[38]
			0.161(8)	0.897(49)	(p,24.5) DWBA		[35]
			0.14(1)		(p,17.8) DWBA		[36]
			0.182(15)	0.859(76)	(α,50.5) CC,SMA	1.372	this work
^{124}Sn			0.119(10)	0.738(60)	(α,50.5) CC	1.038	this work
1.48	2.610		0.116(11)	0.720(70)	(α,50.5) DWBA		this work
		0.0108(15)			(e,150) B_I(L$\to$0)		[32]
			0.138(7)	0.777	(p,24.5) DWBA		[35]
			0.115	0.706(38)	(p,16) CC		[33]
			0.133(20)	0.826(135)	(p,16) DWBA		[25]
		0.0099		0.62	(α,44) A.-B.-DWBA		[24]
		0.18(6)	0.15(2)	0.898(144)	(α,19.5) Coul.Nucl.Interf.		[37]
		0.20(8)			(N14,52.5) Coulomb Excit.		[38]

N o t e. The following method notations are taken: SMA stands for semimicroscopic analysis; DWBA — "distorted-wave Born approximation" calculations; CC — "coupled channels" calculations; A.-B.-DWBA — distorted-wave method with Austern—Blair Coulomb excitation; $B_I(L \to 0)$ — reduced transition probabilities taken from work [32]. Deformation length values δ_2^N for works [27—29] are determined on the basis of corresponding $B(EL)$ values for 2_1^+ states of ^{112,114,120,124}Sn nuclei with $R_C = 1.2\ A^{1/3}$ fm. Errors of the M_n/M_p values constitute (12—14)%.

In work [37], the data on $B(EL)$, β_l, and deformation lengths δ_l^N for 2_1^+ and 3_1^- states of ^{124}Sn nucleus are presented which were obtained from the ADDCS analysis of scattered 19.5-MeV alpha particles in the interference region of the Coulomb and nuclear interactions; in this case, the $B(EL)$ data were by 15% lesser than those measured with the "pure" Coulomb excitation. In [37], the Coulomb and nuclear components are determined separately in the deformation parameters (β_2^C and β_2^N, β_3^C and β_3^N), giving $\beta_2^C > \beta_2^N$ by 8%, and $\beta_3^C > \beta_3^N$ almost by two times. From the data of work [37], we have included, into Table 8, the values of the deformation parameters and deformation lengths calculated using β_l and $R_C = 1.2A^{1/3}$ fm, and consistent with their charge component.

In work [38], the errors of the determination of $B(E3)$ values for ^{114,120,124}Sn, obtained from measurements performed on Coulomb-excited 52.5-MeV ^{14}N ions,

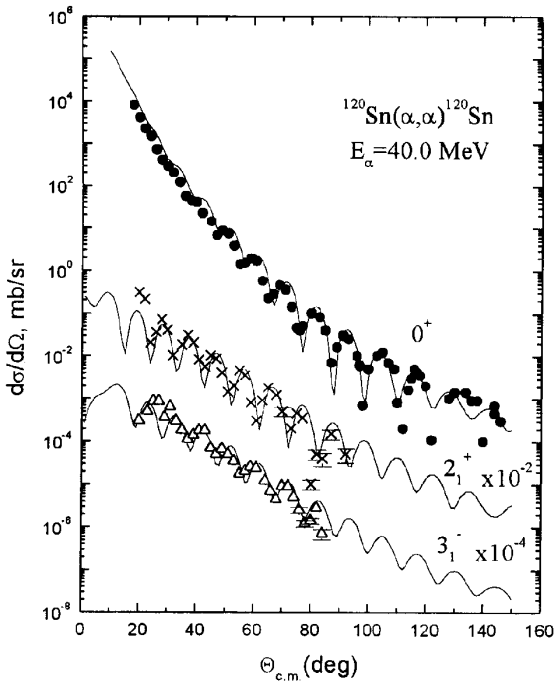

Fig. 3. ADDCS values of elastic and inelastic scattering of alpha particles colliding with a ^{120}Sn nucleus (the symbols show the experimental data [7], and the solid curves — the results of semimicroscopic analysis) with $E_\alpha = 40$ MeV

constitute 40% and are not exhibited in our comparative analysis.

Analysis of the data represented in Table 8 shows that M_n/M_p values for 2_1^+ states of ^{112,114,120,124}Sn nuclei exceed by 1.1 to 1.5 times the corresponding N/Z ratios. Therefore, in the low-lying 2_1^+ states of even Sn isotopes, the neutron component is more deformed than the proton one, and the ratios of these values are more than N/Z corresponding to the collective model concept. It is seen that, for even Sn isotopes, the values of 2_1^+-states' deformation waves obey the relationships $\delta_{em} \leq \delta_{nn'} < \delta_{pp'}$ for ^{112,114,120,124}Sn thus corresponding to the prediction of the "core polarization" model [1] for nuclei with the closed proton shell ($Z = 50$).

It is seen from Table 8 that there is no sufficient amount of reliable data on the charge components for the calculation of the M_n/M_p ratio in 3_1 states of ^{112,114,120}Sn nuclei, so, there is a lack of experiments on the Coulomb-type excitation (or scattering of electrons) of octupole transitions. For the 3_1^- state of ^{124}Sn nucleus, the relationship $1 < M_n/M_p < N/Z$ is met. Within the frame of the same method of analysis (in particular, CCM and DWBA), the relation $\delta_{\alpha\alpha'} < \delta_{pp'}$ is true for the 3_1^- state of ^{120}Sn nucleus, thus corroborating the conclusion of larger deformability of the neutron component as compared with the proton one. At the same time, this inequality is less pronounced for the 3_1^- state of ^{112}Sn nucleus: $\delta_{\alpha\alpha'} \leq \delta_{pp'}$.

The deformation lengths for 2_1^+ and 3_1 states of ^{120,124}Sn nuclei are extracted in [33] basing on the analysis (CCM and DWBA) of the scattering data for polarized 16-MeV protons. In work [33], in which neutron-scattering data [39] were compared, it was found that the relationship $\delta_{nn'} < \delta_{pp'}$ is true for the 2_1^+ state of ^{120}Sn nucleus, thus complying with the prediction of the model [1], whereas, for 2_1^+ state ^{120}Sn nucleus, this relationship is not strict. CCM analysis for the 3_1^- states of ^{120,124}Sn nuclei gives $\delta_{nn'} \approx \delta_{pp'}$.

Note that we do not have information on calculations carried out by the technique of work [1] for octupole states of nuclei, although a need exists in such data.

The authors are grateful to Prof. S.A. Fayans (Russian Scientific Center "Kurchatov Institute") for the access to the data on the microscopic densities of nuclei and the support of our work.

1. *Bernstein A.M., Brown V.R. and Madsen V.A.* // Phys. Lett. B.— 1981.— **103**.— P.255; *Madsen V.A., Brown V.R., Anderson J.D.*// Phys. Rev. Lett.— 1975.— **34**.— P. 1398; Phys. Rev. C.— 1975, **12**.— P.1205.
2. *Rychel A. D., Gyufko R., Van Kruchten B. et al.* // Z. Phys.— 1987.— **A326**.— P.455.
3. *Lund B.J., Bateman N.P.T., Utku S. et al.* // Phys. Rev. C.— 1995.— **51**.— P.635; *Horen D.J., Satchler G.R., Fayans S.A. et al.* // Nucl. Phys. A.— 1996.— **600**.— P.193.
4. *Duisebayev A., Kuterbekov K.A., Kukhtina I.N. et al.* // Yad. Fiz.— 2003.— **66**, N. 4.— P.627—639.
5. *Perey C.M., Perey F.G.* // Atom Data and Nucl. Data Tables. — 1976.— **17**.— P.1.
6. *Firesrone R.B.* Table of Isotopes: 8th Edition. — New York: Wiley, 1999.
7. *Baron N., Leonard R.F., Need Jon L. et al.*// Phys. Rev.— 1966.— **146**.— P.861.
8. *Duisebayev A. Duisebayev B.A., Ismailov K.M., Kuterbekov K.A. et al.* // Proc. MON RK, Nat. Acad. Sci. Rep. of Kazakhstan, Phys. and Math. Series.— 2002.— N. 2.— P.103—109; *Kuterbekov K.A. and Yushkov A.V.* // Pribory Tekhn. Eksp.— 1986.— **3**.— P.35—37.
9. *Perey F.G.*// NBI version.— 1976.
10. *Kuterbekov K.A., Kukhtina I.N., Zholdybayev T.K. et al.* // Preprint JINR E7-2002-220, Dubna, Russia, 2002; *Nolte M., Machner H., Bojowald J.*// Phys. Rev. C.— 1987.— **36**.— P.1312.
11. *Igo G., Wilkins B.* // Phys. Rev.— 1963.— **131**.— P.1251.

12. *Ingemarson A., Nyberg J., Renberg P.U. et al.* // Nucl. Phys. A.— 2000.— **676**.— P.3.

13. *Kunz P.D.*// Computer program DWUCK4 (unpubl.).

14. *Raynal J.*// ECIS-88 (unpubl).

15. *Knyazkov O.M., Kuchtina I.N., Fayans S.A.* // Phys. Part. Nucl.— 1999.— **30**.— P.870.

16. *Satchler G.R.*// Direct Nuclear Reactions. — New York: Oxford University Press, 1983.

17. *Knyazkov O.M., Kuchtina I.N., Fayans S.A.* // Phys. Part. Nucl.— 1997.— **28**.— P.1061.

18. *Ghaudhuri A.K., Basu D.N., Sinha B.* // Nucl. Phys. A.— 1985.— **439**.— P.415.

19. *Fayans S.A., Knyazkov O.M., Kuchtina I.N. et al.* // Phys. Lett. B.— 1995.— **357**.— P.509.

20. *Bolotov D.B., Knyazkov O.M. Kuchtina I.N. et al.* // Yad. Fiz.— 2000.— **63**.— P.1631.

21. *Tanihata I., Kobayashi T., Yamakawa O. et al.* // Phys. Lett. B.— 1988.— **206**.— P.592.

22. *Karcz W., Szmider J., Szymakowski J. et al.* // Acta phys. pol.— 1974.— **B5**.— P.115.

23. *Stelson P.H., McGowan F.K., Robinson R.L. et.al.*// Phys. Rev.— 1968.— **170**.— P.1172.

24. *Bruge G., Faivre J.C., Faraggi H. et al.* // Nucl. Phys. A.— 1970.— **146**.— P.597.

25. *Makofske W., Savin W., Ogata H. et al.* // Phys. Rev.— 1968.— **174**.— P.1429.

26. *Blanket P.J., Blok H.P., Blok J.* // Nucl. Phys. A.— 1980.— **333**.— P.116.

27. *Stelson P.H., Grodzins L.* // Nucl. Data.— 1965.— **1**.— P.21.

28. *Graetzer R., Cohick S.M., Saladin J.X.* // Phys. Rev. C.— 1975.— **12**.— P.1462.

29. *Stelson P.H., McGowan F.K., Robinson R.L. et al.* // Ibid.— 1970.— **2**.— P.2015.

30. *Kumabe I., Ogata H., Kim T.H. et al.* // J. Phys. Soc. Jpn.— 1968.— **25**.— P.14.

31. *Stelson P.H., Robinson R.L., Kim H.J. et al.* // Nucl. Phys.— 1965.— **68**.— P.97.

32. *Barreau P., Bellicard J.B.* // Phys. Rev. Lett.— 1967.— **19**.— P.1444.

33. *Abbot D.J., Clegg T.B., Delaroche J.P.* // Phys. Rev. C.— 1987.— **35**.— P.2028.

34. *Jolly R.K.* // Phys. Rev.— 1965.— **139**.— P.B318.

35. *Beer O., Benay A.E., Lopato P. et al.* // Nucl. Phys. A.— 1970.— **147**.— P.326.

36. *Jarvis O.N., Harvey B.G., Hendrie D.L. et al.* // Ibid.— 1967.— **102**.— P.625.

37. *Vasconcelos S.S., Rao M.N. Ueta N. et al.* // Nucl. Phys. A.— 1979.— **313**.— P.333.

38. *Alkhazov D.G., Gangrskiy Yu.P., Lemberg I.Kh. et al.*// Izv. Akad. Nauk SSSR, Ser. Fiz. [Bull.Acad.Sci. USSR, Phys. Ser.].— 1964.— **28**.— P.232.

39. *Finlay R.W., Rapaport J., Hadizadeh M.N. et al.* // Nucl. Phys. A.— 1980.— **338**.— P.45; *Rapaport J., Mirzaa M., Hadizadeh H. et al.* // Ibid.— 1980.— **341**.— P.56.

Received 19.08.03.
Translated from Russian by A.G. Filin

ФЕНОМЕНОЛОГІЧНИЙ І НАПІВМІКРОСКОПІЧНИЙ АНАЛІЗ РОЗСІЯННЯ АЛЬФА-ЧАСТИНОК З ЕНЕРГІЄЮ 50 МеВ І СТРУКТУРА ПАРНИХ ІЗОТОПІВ ОЛОВА

К.А. Кутербеков, І.Н. Кухтіна, Б.М. Садиков, Є.І. Ісматов

Р е з ю м е

Виконано феноменологічний і напівмікроскопічний аналіз експериментальних даних з пружного і непружного розсіяння α-частинок з енергією близько 50 МеВ на ядрах ^{112,114,120,124}Sn (разом з наявними даними з повних перерізів реакцій) в рамках моделі оптичного потенціалу, методів спотворених хвиль та зв'язаних каналів. Для низькоенергетичних 2^+_1- та 3^-_1-станів отримано відповідні значення параметрів деформації, деформаційних довжин, відношень нейтронних і протонних мультипольних елементів переходів, а також проведено порівняння визначених значень параметрів з літературними даними для інших типів налітаючих частинок.